Effect of precipitate on yield strength of ferritic/martensitic steel exposed to 650 °C liquid sodium

Tae Yong Kima, Sang Hun Shin[b], Jeonghyeon Lee[a] and Ji Hyun Kim[a]*
[a] *School of Mechanical and Nuclear Engineering, Ulsan National Institute of Science and Technology (UNIST), Ulju-gun, Ulsan 44919, Republic of Korea*
[b]*Korea Atomic Energy Research Institute (KAERI), Yuseong-gu, Daejeon 34057, Republic of Korea*
[*]*Corresponding author: kimjh@unist.ac.kr*

1. Introduction

Liquid sodium used with coolant of Ultra-long Cycle Fast Reactor(UCFR) has good thermal conductivity (87.1 W/m·K) and specific heat (1.38kJ/kg). The low viscosity and wide range of liquid temperature (97.8~883 ℃) which give large margin for reactor design can provide safety for operation. Ferritic/martensitic steels(FMS) which are used as one of cladding and structure materials in UCFR, have high creep strength at 600~650℃, low expansion coefficient, and dimensional stability with irradiation-induced void swelling in circumstance of fast neutrons compared to austenitic stainless steel [1-3]. However, as exposed to high temperature liquid sodium during the design life time (30 to 60 years), the surface of FMS experienced Cr-depletion and decarburization by dissolution of components into sodium and formed oxidations by reacting with sodium [4]. This changes chemical compositions of inter-surface and effects on behavior of precipitations. This change can cause a degradation of mechanical strength of structure material of UCFR. Therefore, we should consider long-term compatibility with sodium and study about life prediction.

The research about FMS on effects of long term exposure in liquid sodium at 650 ℃ involve analysis of yield strength by change of microstructure, solid solution hardening and precipitation hardening. It shows how this three parts occupy total yield strength respectively and change over time.

In a specific procedure, the microstructure and the surface phenomenon of FMS (Gr. 92) that are exposed to liquid sodium at 650℃, 20 ppm oxygen and are aged in high pure Argon gas environment to express bulk have been investigated by using scanning electron microscope (SEM) and transmission electron microscope (TEM) [5-6].

2. Experimental

The test material in this study is ASTM A182 Gr.92 steel, which contains approximately 9 wt. % of chromium and 2 wt. % of tungsten. Chemical composition of this material is shown in Table. I. Tubes of Gr.92 were manufactured by hot extrusion and multiple passes of cold drawing. The tubes were normalized at 1080 ℃ for 6 min and tempered at 800℃ for 6 min so as to develop a tempered martensite structure [7].

Table I. Chemical compositions in wt.% of Gr.92 alloy (wt. %).

C	Si	Mn	Cr	Ni	Mo	W
0.087	0.21	0.41	8.69	0.13	0.38	1.62
V	Nb	Cu	N	B	P	S
0.18	0.07	0.10	0.046	0.002	0.012	0.002

There are two kind of Gr. 92 cladding tubes. Some were exposed to liquid sodium at 650 ℃, saturated oxygen (3871 ppm calculated by [8]) for 1583 hours. The others were exposed to 650 ℃ liquid sodium at initially 20 ppm oxygen for 1512 h and then at saturated for 1583 hours, totally 3095 hours. As a comparative control to test the effect of sodium, other Gr. 92 cladding tubes were encapsulated in a 99.99 % pure Ar environment, and then kept in a 650 ℃ muffle furnace for 1601 hours or 2973 hours.

3. Results

3.1 SEM analysis

Figure 1 (a) and (b) show cross-section of specimens which exposed to 650 ℃ sodium for 1583 hours and 3095 hours. Oxidations are found from Fig. 1. From Fig. 3, chromium reacting with sodium forms $NaCrO_2$ oxides of 10~20 μm size on the surface up to 40 μm. Intergranular corrosion occurred through the sodium oxide region about 40 μm in both specimens. In Fig. 1 (b), after exposed to sodium for 3095 h, more pores can be found, and corrosion occurred more severe. From Fig. 3, it can be found Cr depletion and decarburization from 40 μm to 50 μm section.

Thorough EPMA mapping, it shows that other elements like C, Mo, W not only Cr from surface to a depth of 50 μm are dissolved toward sodium. In case of fuel cladding having 570 μm thickness, it would exert a strong influence on mechanical properties of fuel cladding, because 50 μm forms 9 % of total thickness.

Fig. 2 (a) and (b) is SEM image of cross section of Gr.92 specimen thermally aged during 1601 hours and 2973 hours in 650 ℃ Ar-gas environment. There are no forming oxide and intergranular corrosion unlike sodium environment. There is no change also in the size of grain regarding between Fig. 1 and Fig.2. However, sub-grains

involved in 10 μm sized grain, called tempered martensite structure, have changed their size. As-received specimens have uniform tempered martensite structure across the specimens. It has similar size from 0.5-1 μm [9]. Tempered martensite structure of sodium exposed specimens and Ar-gas exposed specimens, but on the other, have been coarsened with 10 μm.

During exposed to high temperature at sodium or Ar-gas, annealed lath structure as well as coarsening of tempered martensite structure affects reduction of mechanical properties.

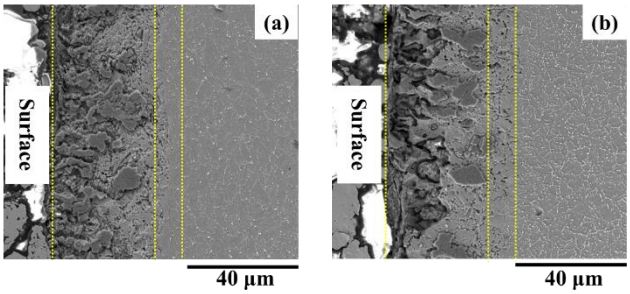

Figure. 1. SEM images of cross-section of specimen after exposure to 650 ℃ sodium for (a) 1583 h and (b) 3095 h [7].

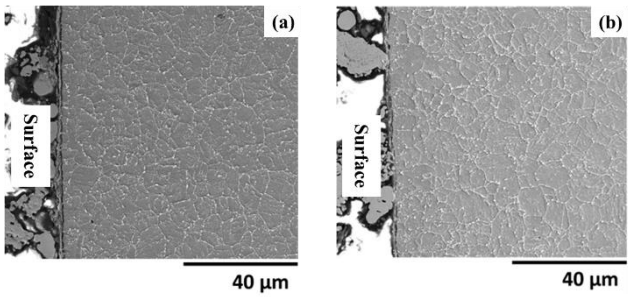

Fig. 2. SEM images of cross-section of specimen after exposure to 650 ℃ Ar-gas for (a) 1601 h and (b) 2973 h [7].

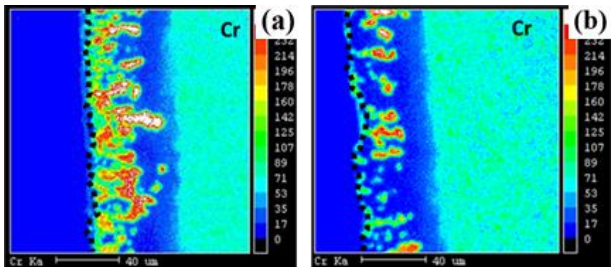

Fig. 3. EPMA X-ray mapping of Gr. 92 specimen which was exposed to Na for (a) 1583 h and (b) 3095 h at 650 ℃ [7].

3.2. TEM analysis

Thorough TEM analysis, size and density of precipitations are calculated. Fig. 4 is TEM images of carbon extraction replicas of specimens of (a) as-received, (b) 650 ℃ sodium exposed for 3095 hours and (c) 650 ℃ Ar-gas exposed for 2973 hours. Surely, another carbon extraction replicas of specimens exposed to 650 ℃ sodium for 1583 hour and 650 ℃ Ar-gas for 1601 hour.

The number density of precipitates of each specimen are charted at Table II.

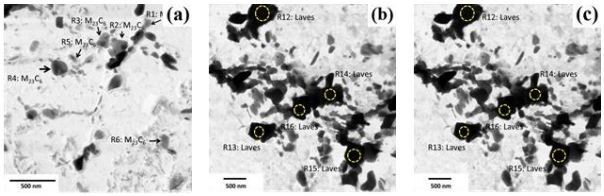

Fig. 4. TEM images of carbon replicas for precipitates in the specimens (a) as-received, (b) 650 ℃ sodium exposed for 3095 h, (c) 650 ℃ Ar-gas exposed for 2973 h.

Table II. the number of precipitates (#/μm2)

	As-receive	Na-1583 h	Ar-1601 h	Na-3095 h	Ar-2973 h
ρ	2.63	1.40	1.82	1.04	1.52

And the size of precipitates calculated from carbon extended replicas are charted at Table III. However, the calculated values are size that cross section of precipitates is cut random position like right three circles of Fig. 5. So, the real diameter of precipitates need to modify calculated average diameter of precipitates from eq. 2 and 3. Finally, we can calculate real size of precipitation from Table IV.

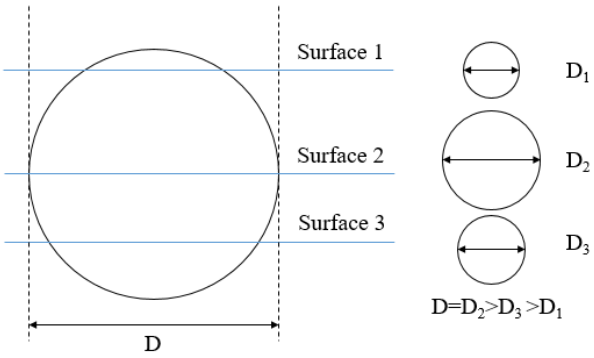

Fig. 5. Schematic diagram of cross section of precipitate by each cutting surface.

Simply, average diameter is calculated like:

$$D_{avg} = \frac{\Sigma D_n}{n} \quad (1)$$

And, the relation equation between average diameter(D_{avg}) and real diameter(D) of precipitate:

$$D_{avg} = 2\int_{-\frac{D}{2}}^{\frac{D}{2}} \sqrt{(\frac{D}{2})^2 - x^2} * \frac{dx}{D} \quad (2)$$

$$D_{avg} = \frac{\pi}{4} D \quad (3)$$

Table III. size of precipitates calculated by TEM image

	As-receive	Na-1583 h	Ar-1601 h	Na-3095 h	Ar-2973 h
D	47	113	143	218	171

Table IV. real size of precipitates

	As-receive	Na-1583 h	Ar-1601 h	Na-3095 h	Ar-2973 h
D	59.8	144	182	278	218

4. Discussion

Mechanical properties like yield strength are depend on grain size effect(Hall-Petch), solid solution hardening and precipitation hardening. Therefore, we have to analysis change of microstructure for grain size effect(Hall-Petch), size and concentration of elements for solid solution hardening, and size and density of precipitations for precipitation hardening. First, each part is calculated respectively. So, we can evaluate the change of each part. Finally, considering relation of each three part with total yield strength, it shows how each fraction of Hall-Petch, solid solution hardening and precipitation hardening on yield strength are changed as time passes.

4.1. Effect of microstructure for yield strength

FMS have uniform tempered martensite structure composed with 0.5-1 μm sub-grain. it can make FMS have strong yield strength. However, the structure was annealed by high temperature while exposed to sodium or Ar-gas. The annealed structure is coarsened with 10 μm size. Through Hall-petch equation, we can evaluate yield strength by microstructure. However, we can't evaluate total yield strength made only by microstructure just yet. Because coefficient for Hall-Petch equation can't calculate without considering yield strength component; solid solution hardening and precipitation hardening. However, we can calculate reduction fraction of yield strength of microstructure by change of diameter. For that, we need to know Hall-Petch equation:

$$\sigma_{y,H.P.} = \frac{k_{H.P.}}{\sqrt{D}} \quad (4)$$

$k_{H.P.}$ is coefficient of Hall-Petch equation and D is size of microstructure involved in tempered martensite structure.

Size of microstructure of as-received specimens is about 0.5 μm. The size is increased with 10 μm exposed to sodium for 1583, 3095 hours and Ar-gas for 1601, 2973 hours. This means that yield strength is decreased with increasing size of microstructure. So, reduction rate of exposed specimens compared with as-received specimens is calculated like:

$$\frac{\sigma_{y,exposed}-\sigma_{y,as-received}}{\sigma_{y,as-received}} = \frac{\sqrt{D_{as-received}}}{\sqrt{D_{exposed}}} - 1 \quad (4)$$

There is reduction of 77.6% on yield strength of microstructure by high temperature. This is large value but we need to evaluate the value compared with total yield strength.

4.2 Effect of solid solution for yield strength

Solid solutes act as hinder of dislocation moving. Therefore, many solid solutes increase yield strength. However, the weight of the hinder effect varies in solute size. If any solute size (Cr, Ni etc.) is similar with base metal (Fe), the hinder effect is low. On the other hand, if there is big difference in size between solute (C, W etc.) and base metal (Fe), the hinder effect is large. the reason is that large difference in size make large strain near them. Therefore, the strain interacts with dislocation difficult to move. The maximum interaction force(f_m) between a dislocation and a solute atom is [10]:

$$f_m = \frac{Gb^2}{120}\varepsilon_b \quad (5)$$

G is shear modulus with 82.19 GPa and ϵ_b is strain by burgers vector of dislocation [11]. The strain calculated from eq. 6. c is concentration of solute. By this component, we can use Nabusch-Nabarro model for solid solution hardening with eq. 7 [11].

$$\varepsilon_b = \frac{1}{G} * \frac{dG}{dc} \quad (6)$$

$$\sigma_{y,solutions} = \frac{(2wf_m^4c^2)^{\frac{1}{3}}}{2b^{\frac{7}{3}}(Gb^2)^{\frac{1}{3}}} = 18454 * \varepsilon_b^{\frac{4}{3}} * c^{\frac{2}{3}}(MPa) \quad (7)$$

From this equation, the yield strength by solid solutions is calculated with Table V.

Table V. yield strength calculated by solid solution

	As-receive	Na-1583 h	Ar-1601 h	Na-3095 h	Ar-2973 h
σ_y	476	378	413	376	408

As-received specimens have largest yield strength with 475 MPa. But, specimens exposed to sodium decrease 99MPa with 376 MPa. And specimens exposed to Ar-gas decrease 67 MPa with 408 MPa. Decreasing of yield strength by solid solution is little less than that by changing of microstructure. Nevertheless, decreasing solid solution is considerable.

4.3 Effect of precipitation for yield strength

Fixed precipitation also effects on moving of dislocations and sub-grain boundaries like Fig. 6. Over time, various precipitations like $M_{23}C_6$ and Laves-phase nucleate and grow thermodynamically. Therefore, hardening by precipitation increases with increasing of size and density of precipitations.

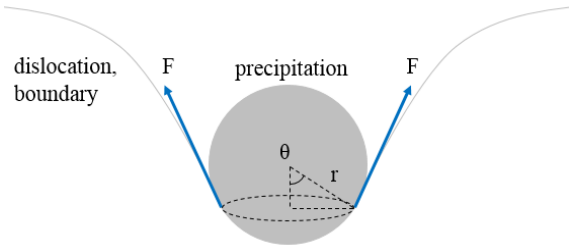

Fig. 6. Schematic diagram of interaction between precipitation and dislocation or sub-grain boundary.

Surface energy(γ) between precipitation and some boundaries is hinder force on moving of boundaries. From experiment result, surface energy is 0.005 J/m^2 [12]. If there is a precipitation having 'r' with radius and 'θ'

angle between central axis of precipitation and normal axis to boundary, the precipitation exerts a force is expressed with eq. 8. Assuming that all precipitation exerts maximum force to boundaries, total precipitation force in material is expressed with eq. 9. n_i is a number of precipitations per unit area. The total force is calculated with Table VI. Precipitation hardening is proportional to the total force by precipitations. So, precipitation hardening is expressed by eq. 10. k_p is coefficient of yield strength by precipitation.

$$F = \pi r \gamma \sin 2\theta \quad (8)$$

$$P = \Sigma F_i \cdot n_i \quad (9)$$

$$\sigma_{y,solutions} = k_p * P \quad (10)$$

Table VI. Precipitation pressure (Pa)

	As-receive	Na-1583 h	Ar-1601 h	Na-3095 h	Ar-2973 h
σ_y	102	103	219	193	216

4.4 Total yield strength

From above three yield strength with the coefficient, the fraction of each yield strength can be evaluated. The total yield strength can be expressed by eq. 11. And total yield strength by eq. 11 is showed in Table VII.

Through this value, k_p and $k_{H.P}$ is 1.54×10^5 and 79.9, respectively. From Table VIII, after exposing, there is no evident change of yield strength by solid solution and microstructure at each environment. However, at sodium environment, yield strength by precipitation increases by two times over time, although Ar-gas environment is remained. It might be resulted from coarsening at Ar-gas environment while there is not enough precipitation to coarsen themselves at sodium environment. So, yield strength by precipitation can increase continuously.

$$\sigma_y = k_p * P + 18454 * \Sigma \varepsilon_{b,i}^{\frac{4}{3}} c_i^{\frac{2}{3}} + \frac{k_{H.P.}}{\sqrt{D}} \quad (11)$$

Table VII. Total yield strength(MPa)

	As-receive	Na-1583 h	Ar-1601 h	Na-3095 h	Ar-2973 h
σ_y	618	419	472	431	467

Table VIII. Total yield strength(MPa)

	As-receive	Na-1583 h	Ar-1601 h	Na-3095 h	Ar-2973 h
Precipitation	15.8	15.8	33.7	29.7	33.3
Solid Solution	476	378	413	376	408
Hall-Petch	126	25.2	25.2	25.2	25.2

3. Conclusions

When specimens were exposed to 650 ℃ liquid sodium for 1583, 3095 hours and Ar-gas 1601, 2973 hours, mechanical properties of materials were analyzed quantitatively. After experiment, NaCrO2 oxidation was formed on the surface of Gr.92 at sodium environment. Also, change of microstructure, dissolution of elements, and nucleation and growth of precipitation was raised. During exposed to high temperature at sodium or Ar-gas, annealed lath structure as well as coarsening of tempered martensite structure affects reduction of mechanical properties. And dissolution of elements results in reduction of solid solution hardening. This phenomenon was raised before 1500 hours. So, change of mechanical properties by them is barely observable. However, at sodium environment, yield strength by precipitations increases over time, because there is enough room for nucleation and growth of precipitations. On the other hand, at Ar-gas environment, yield strength is remained by coarsening of precipitation.

REFERENCES

[1] S.H. Shin, J.J. Kim, J.A. Jung, K.J. Choi and J.H. Kim, Development of experimental system for materials compatibility test for ultra-long cycle fast reactor (UCFR), NFSM, American Nuclear Society, 2012, Chicago, IL.
[2] S. H. Shin et al., Corrosion behavior and microstructural evolution of ASTM A182 Grade 92 steel in liquid sodium at 650C, Corrosion Science, Vol.97, pp.172-182, 2015.
[3] S. H. Shin et al., A study on corrosion behavior of austenitic stainless steel in liquid metals at high temperature, Journal of Nuclear Materials, Vol.422, pp.92-102, 2012.
[4] H. L. klueh and D. R. Harries, High-Chromium Ferritic and Martensitic Steels for Nuclear Applications, American Society for Testing and Materials, pp.33, 2001.
[5] S. H. Shin et al., Model of liquid gallium corrosion with austenitic stainless steel at a high temperature, Journal of Nuclear Materials, Vol.450, pp.314-321, 2014.
[6] S. W. Lee, S. D. Park, S. Kang, S. H. Shin, J. H. Kim and I. C. Bang, Feasibility study on molten gallium with suspended nanoparticles for nuclear coolant applications, Nuclear Engineering and Design, Vol.247, pp.147-159, 2012.
[7] S.H. Shin, J.H. Kim and J.H. Kim, Effect of Aging ASTM A182 Grade 92 Steel on Corrosion Behavior and Microstructural evolution in Liquid Sodium at 650℃, Corrosion science, Vol.97, pp.172-182, 2015.
[8] R. L. Eichelberger, THE SOLUBILITY OF OXYGEN IN LIQUID SODIUM : A RECOMMENDED EXPRESSION, A DIVISON OF NORTH AMERICAN ROCKWELL CORPORATION, pp.1-21, Nov.1, 1968.
[9] J. H. Kim, J. M. Kim, S. H. Kim, and C. B. Lee, Microstructural and Mechanical Property Evaluation of the Ferritic-Martensitic Steel under Liquid Sodium Environment, Kor. J. Met. Mater., Vol.48, pp.914-921, 2010.
[10] M. Z. BUTT et al., Review Solid-solution hardening, Journal of Materials Science, Vol.28, pp.2557-2576, 1993.
[11] H. Seurin, J. Zander and R. Sandstrom, Modelling solid solution hardening in stainless steels, Materials Science and Engineering, Vol.4115, pp.66-71, 2016.
[12] J. J. HOYT and S. SPOONER, THE SURFACE ENERGY OF METASTABLE Al_3Li PRECIPITATES FROM COARSENING KINETICS, Acta Metallurgica et Materialia, Vol.39, pp.689-693, 1991.
[13] D. A. Porter et al., Phase transformations in metals and alloys – third edition, pp.145, 2009.